

Structure and electronic properties of amorphous LaAlO₃ film on In_{0.53}Ga_{0.47}As

N. Goel, W. Tsai, and C. M. Garner
Intel Corporation, Santa Clara, California 95052

Y. Sun and P. Pianetta
Stanford Synchrotron Radiation Laboratory, Stanford University, Stanford, California 94205

M. Warusawithana and D.G. Schlom
Department of Materials Science and Engineering, Pennsylvania State University, University Park, Pennsylvania 16802-5005

H. Wen, C. Gaspé, J.C. Keay, and M.B. Santos
Homer L. Dodge Department of Physics and Astronomy, The University of Oklahoma, Norman 73019

L.V. Goncharova, E. Garfunkel, and T. Gustafsson
Laboratory for Surface Modification, Rutgers University, 13, Frelinghuysen Rd., Piscataway, New Jersey 08854

The valence and conduction band offsets between an amorphous LaAlO₃ dielectric and a *n*-In_{0.53}Ga_{0.47}As (001) layer prepared by molecular-beam deposition have been measured using synchrotron radiation photoemission spectroscopy. The valence and conduction band offsets at the post-deposition annealed LaAlO₃/InGaAs interface are $\sim 3.1 \pm 0.1$ eV and $\sim 2.35 \pm 0.2$ eV, respectively. The band gap of LaAlO₃, as determined by Al *2p* and O *1s* core-level energy loss spectra, is $\sim 6.2 \pm 0.1$ eV. Within the resolution of the medium energy ion scattering technique, no interfacial oxide layer is seen between the InGaAs and the 3.6 nm-thick LaAlO₃.

As the size of complementary metal-oxide-semiconductor (CMOS) transistors continues to be reduced, high dielectric constant (high- κ) materials are being sought to replace the silicon dioxide (SiO₂) as gate dielectric. High- κ material allows thicker physical thickness of gate oxides for equivalent electrical oxide thickness (EOT) and thus lower gate leakage. Moreover due to fundamental limits to the scaling of Si, high mobility and smaller band gap III-V channel materials¹ based on indium gallium arsenide (In_{*x*}Ga_{1-*x*}As) and indium antimonide (InSb), are currently being actively investigated for future logic technology generations. In _{≥ 0.53} Ga _{≤ 0.47} As and InSb high electron mobility transistors (HEMTs) with highly promising device characteristics such as excellent drive current and gate delay characteristics, have already been demonstrated.^{2,3} To reduce gate leakage and improve the $I_{\text{on}}/I_{\text{off}}$ ratio in these devices, it is important to integrate a good quality dielectric in the gate stack. Besides the need to have a high- κ value for this dielectric, it is critical to have sufficient valence and conduction band discontinuities between the insulator and the semiconductor to act as a barrier for both electron and hole injection.^{4,5} Furthermore, to achieve EOT < 1 nm it is essential to have an abrupt interface without lower- κ dielectric between the high- κ gate dielectric and the semiconductor.

Due to several promising characteristics including high- $\kappa \sim 16$,^{6,7} good thermal stability⁸ and reasonable band offsets⁷ (> 1 eV) with Si as well as < 0.2 Å of SiO₂ at the interface between the amorphous LaAlO₃ and silicon⁹, observed in molecular-beam deposited amorphous LaAlO₃/Si MOS structures⁶⁻⁹, we have begun to explore the possibility of its inclusion as the gate dielectric in InGaAs-based devices. A comprehensive thermodynamic analysis of the stability of binary oxides in contact with III-V semiconductors¹⁰ indicates that there are no expected reactions between La₂O₃ or Al₂O₃ with GaAs or InAs, and thus, LaAlO₃ is expected to form a stable interface with InGaAs. The stability of the

LaAlO₃/In_{0.53}Ga_{0.47}As interface in devices annealed up to 500 °C and the absence of interfacial oxide between LaAlO₃ and InGaAs has been verified within the resolution of high-resolution transmission electron microscopy (HRTEM), high angle annular dark-field scanning TEM (HAADF-STEM), electron energy loss spectroscopy (EELS), and energy dispersive x-ray spectroscopy (EDXS) techniques.¹¹ We have demonstrated LaAlO₃ MOS capacitors have reasonable electrical characteristics such as considerably low frequency dispersion, < 40 mV hysteresis and reasonably low leakage current density ($\sim 5 \times 10^{-4}$ A/cm²) for a gate stack with a capacitance equivalent thickness (CET) of ~ 1.3 nm.¹¹ Spectroscopic ellipsometry and HRTEM indicated that the as-deposited dielectric film becomes denser and CET increases with annealing.¹¹

In this paper we report the physical structure and electronic properties of molecular-beam deposited thin amorphous LaAlO₃ on *n*-In_{0.53}Ga_{0.47}As as measured by medium-energy ion scattering (MEIS) and synchrotron radiation photoemission spectroscopy (SRPES). Since this dielectric has promising electrical characteristics, a better understanding of the structure and electronic properties of this dielectric-semiconductor interface is also needed.

A 150-nm thick Si-doped In_{0.53}Ga_{0.47}As epi layer was deposited on a 100 nm-thick *n*-In_{0.52}Al_{0.48}As buffer layer grown on *n*⁺ InP (001) substrates in a GEN II molecular beam epitaxy (MBE) system. In order to minimize the defect density as well as native oxide formed at the interface between the dielectric and III-V layer, the InGaAs samples were capped with an amorphous arsenic layer.¹² The samples were then shipped from the University of Oklahoma to Penn State University in a vacuum jacket where the arsenic cap was desorbed in an EPI 930 MBD system in the absence of arsenic overpressure. Amorphous LaAlO₃ was then deposited at 80 °C substrate temperature by a technique described previously.^{6-9,11}

The electronic properties such as valence band offset (ΔE_V) and conduction band offset (ΔE_C) between LaAlO_3 and $n\text{-InGaAs}$ were determined by photoemission spectra taken on Beam Line (BL) 8-1 (photon energy range of 30–170 eV) and 10-1 (photon energy range of 200 – 1200 eV) at the Stanford synchrotron radiation laboratory (SSRL). The tunability of the photon energy using synchrotron radiation (SR) enables high surface sensitivity by selecting photon energies that provide electron energies with minimum escape depths of ~ 0.5 nm. The Gaussian broadening by the analyzer and the beamline is about 0.15 eV. The medium energy ion scattering measurement (MEIS) was performed, using instrument described in details elsewhere,^{13,14} with a double channeling geometry in the InGaAs $[\bar{1}\bar{1}2]$ scattering plane, the incoming beam aligned with a $[100]$ channeling direction and the detector axis aligned with an InGaAs $[111]$ axis. H^+ beam of the 130 keV energy and scattering angle of 125.3° were typically used.

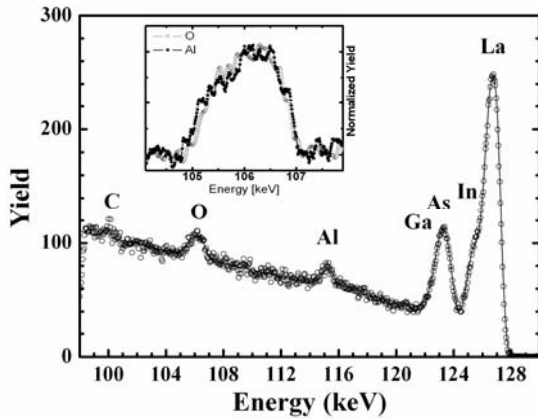


FIG. 1. MEIS energy spectrum (dots) of a 3.6 nm-thick amorphous LaAlO_3 film on InGaAs after post dielectric *in-situ* anneal at 440°C . The quantitative model data (line), where an oxide-free interface is assumed, is also shown. In the insert, the overlap of the Al peak with the O peak is shown. (normalized, background subtracted).

The MEIS spectrum of a 3.6 nm-thick LaAlO_3 film on InGaAs , Fig. 1, has well separated oxygen, aluminum, gallium/arsenic, and lanthanum/indium peaks. Backscatter model analysis is consistent with an abrupt interface between the LaAlO_3 and InGaAs , assuming LaAlO_3 film stoichiometry $\text{La} : \text{Al} : \text{O} = 1 : 1.1 : 3.1$, within the 0.2 - 0.3 nm resolution of this analysis. Furthermore, nearly identical Al and O profiles, Fig. 1 insert, indicate the absence of another oxygen-containing phase at the interface. Thus, no interfacial oxide layer is observed for the as-deposited LaAlO_3 (not shown) or after anneals at 440°C (Fig. 1) or 500°C (not shown).

The model proposed by Kraut et al.^{15,16} was used to determine ΔE_V between amorphous LaAlO_3 and $\text{In}_{0.53}\text{Ga}_{0.47}\text{As}$.

$$\Delta E_V = (E_{\text{As}3d} - E_V)_{\text{InGaAs}} - (E_{\text{Al}2p} - E_V)_{\text{LaAlO}_3} - (E_{\text{As}3d} - E_{\text{Al}2p})_{\text{LaAlO}_3/\text{InGaAs}} \quad (1)$$

where, $E_{\text{As}3d}$, and $E_{\text{Al}2p}$ were the core level positions, E_V for InGaAs and LaAlO_3 were the valence-band maximum (VBM) of bulk materials, combined with the core level difference of the heterojunction ($\text{LaAlO}_3/\text{InGaAs}$). The $\text{LaAlO}_3/\text{InGaAs}$ samples were either as-deposited or annealed at 440°C and 500°C in a UHV chamber to remove the adsorbed carbon compounds and hydroxyls (OH) on the film surface.⁷ To remove the native oxide from the bulk InGaAs , the sample

was cleaned in dilute HF prior to loading in to the chamber and annealed at 200°C in UHV for a few minutes to eliminate the elemental arsenic (As-As) contribution¹⁷ on the surface of the sample and its contribution to the reference As $3d$ peak. The As $3d$ signal of clean bulk InGaAs consists of a doublet with As $3d_{3/2}$ and a As $3d_{5/2}$ peak where As $3d_{3/2}$ is at higher binding energy (not shown here). The core levels and valence bands of interest were measured with a photon energy source of 140 eV at normal incidence with the electron energy analyzer pass energy of 11.75 eV.

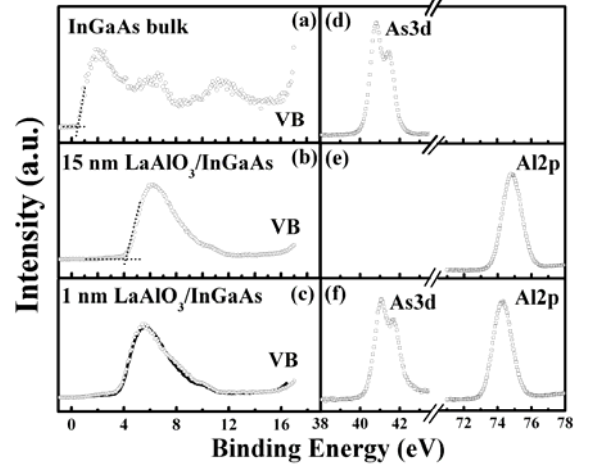


FIG. 2. Valence-band and shallow core level synchrotron radiation photoelectron spectra for bare bulk $n\text{-In}_{0.53}\text{GaAs}$ (001) (a and d), a 15 nm-thick amorphous LaAlO_3 film (b and e), and a 1 nm-thick $\text{LaAlO}_3/\text{InGaAs}$ heterojunction (c and f). In (c), the simulated VB spectrum (solid line) is compared with the experimental VB spectra (open circles) for the as-grown $\text{LaAlO}_3/\text{InGaAs}$ heterojunction.

The valence-band (VB) spectra and core levels, Fig. 2, for clean bulk InGaAs (no dielectric), 15 nm-thick LaAlO_3 and 1 nm-thick amorphous $\text{LaAlO}_3/\text{InGaAs}$ heterojunctions were used to establish the valence band offsets. For clarity, each spectrum is plotted with the maximum intensity scale for the respective peak. The VBM energies for clean InGaAs , Figs. 2(a) and 2(d), and as-deposited LaAlO_3 , Figs. 2(b) and 2(e), were determined to be 0.37 ± 0.05 eV and 3.69 ± 0.05 eV, respectively by the linear extrapolation method.¹⁸ The measured VBM, Al $2p$ and As $3d$ core level energy for as-deposited and annealed dielectric samples as well as bulk clean InGaAs are summarized in Table I. The ΔE_V between LaAlO_3 and $\text{In}_{0.53}\text{Ga}_{0.47}\text{As}$ was then calculated by inserting these values in Eq. (1) and is also listed in Table I. Comparison of the LaAlO_3 (1nm thick)/ $n\text{-InGaAs}$ annealed interface spectra, Fig. 2(c) dots, with a simulated VB spectrum (line) suggests that there is negligible contribution of any interfacial layer. The simulated VB spectrum was produced by shifting and summing the VB data for the annealed 15 nm-thick LaAlO_3 and clean bulk InGaAs .¹⁸

Sample	UHV T _{anneal} (°C)	$E_{\text{As}3d}$ (eV)	$E_{\text{Al}2p}$ (eV)	E_{VBM} (eV)	ΔE_V (eV)	ΔE_C (eV)
Bulk clean InGaAs	200	40.8	-	0.37 ± 0.05	-	-
15 nm $\text{LaAlO}_3/\text{InGaAs}$	as-deposited	-	75.15	3.69 ± 0.05	2.95 ± 0.1	2.5 ± 0.2
	440	-	74.75	4.21 ± 0.05	3.097 ± 0.1	2.35 ± 0.2
	500	-	74.7	4.19 ± 0.05	3.085 ± 0.1	2.36 ± 0.2
1 nm $\text{LaAlO}_3/\text{InGaAs}$	as-deposited	41.04	74.52	-	-	-
	440	41.05	74.25	-	-	-
	500	40.95	74.15	-	-	-

TABLE I. Summary of core levels, valence bands, conduction band offsets (ΔE_C) and valence band offsets (ΔE_V) for bulk n - $\text{In}_{0.53}\text{Ga}_{0.47}\text{As}$, as-deposited and UHV-annealed amorphous LaAlO_3 films on n - $\text{In}_{0.53}\text{Ga}_{0.47}\text{As}$.

The band gap values of the oxide-based dielectric materials can be obtained from the photoelectron spectra by using the onsets of the electron energy loss signal for the Al $2p$ and O $1s$ core level peak.¹⁹ The onset of the energy-loss spectrum, Fig. 3, was defined by linearly extrapolating the segment of maximum negative slope to the background level¹⁷ and hence the band gap was determined. The band gap of the annealed amorphous LaAlO_3 , (E_g) $_{\text{LaAlO}_3}$, for both 9.5 and 15 nm thick LaAlO_3 was thus determined to be 6.2 ± 0.1 eV. A similar value was obtained for as-grown LaAlO_3 (not shown). Within the experimental errors, this result agrees with the earlier reported values determined by spectroscopic ellipsometry on amorphous LaAlO_3 where the dielectric was also deposited by a similar process⁷ as well as thick amorphous LaAlO_3 deposited by alternate techniques.²⁰

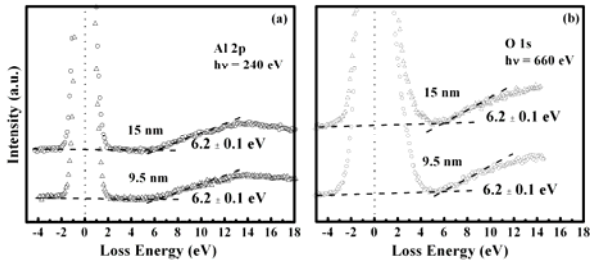


FIG. 3. Energy loss spectra of (a) Al $2p$ and (b) O $1s$ photoelectrons of 9.5 and 15 nm-thick amorphous LaAlO_3 films post deposition annealed at 440°C . The two curves in each plot are deliberately offset along the intensity axis for clarity. The band gap was determined by linear extrapolation, shown by dashed lines.

From the VBM and E_g values, the CBO between LaAlO_3 and InGaAs given by,

$$\Delta E_C = (E_g)_{\text{LaAlO}_3} - (E_g)_{\text{InGaAs}} - \Delta E_V \quad (2)$$

is calculated for unannealed and *in situ* annealed samples, listed in Table I. Here, $(E_g)_{\text{InGaAs}}$ is the band gap of $\text{In}_{0.53}\text{Ga}_{0.47}\text{As}$ (0.75 eV). We determine the band offsets to be $\Delta E_V = 3.1 \pm 0.1$ eV and $\Delta E_C = 2.35 \pm 0.2$ eV for annealed LaAlO_3 on n - $\text{In}_{0.53}\text{Ga}_{0.47}\text{As}$ (001).

For comparison, reported experimental values of ΔE_V and ΔE_C between amorphous LaAlO_3 and Si are $\sim 3.2 \pm 0.1$ eV and 1.8 ± 0.2 eV, respectively, where LaAlO_3 was deposited by similar technique.⁷ Using the charge neutrality levels method, the ΔE_C and ΔE_V of LaAlO_3 have been calculated to be 1.5 and 2.6 eV with GaAs and 2.5 and 2.7 eV with InAs, respectively.⁴ Considering the band gap of LaAlO_3 used for calculations (5.6 eV, corresponding to the band gap of crystalline LaAlO_3)²¹ is different than band gap of amorphous LaAlO_3 (6.2 eV), the experimental offset values obtained on $\text{In}_{0.53}\text{Ga}_{0.47}\text{As}$ are close to the interpolated calculated values. Since the experimentally deduced band offset values are >1 eV, a requirement for a gate oxide to act as a barrier to both electrons and holes,^{4,5} amorphous LaAlO_3 appears to be a plausible candidate for integration with InGaAs for MOS devices.

In summary, we have used a combination of shallow core-level and valence band photoemission measurements to directly determine the valence and conduction band offsets at

the amorphous LaAlO_3/n - $\text{In}_{0.53}\text{Ga}_{0.47}\text{As}$ interface. The band gap of the dielectric film as measured by Al $2p$ and O $1s$ energy loss spectra, is $\sim 6.2 \pm 0.1$ eV. Within the resolution of MEIS, no interfacial oxide layer was observed between InGaAs and a 3.6 nm-thick LaAlO_3 overlayer. These characteristics make LaAlO_3 a promising candidate for InGaAs -based devices for logic application.

ACKNOWLEDGMENT

Part of this study was carried out at the Stanford Synchrotron Radiation Laboratory (SSRL), a national user facility operated by Stanford University on behalf of the U.S. Department of Energy, Office of Basic Energy Sciences. The authors are grateful to the SSRL staff for their support, Prof. M. Hong (NTHU) for discussion, and Intel for funding.

REFERENCES

1. R. Chau, S. Datta, and A. Majumdar, Tech. Digest, IEEE Compound Semiconductor Integrated Circuit Symposium (2005), pp. 17-20.
2. D.-H. Kim, J. A. del Alamo, J. H. Lee, and K. S. Seo, Tech. Dig.- Int. Electron Devices Meet. 2005, 767; D.-H. Kim and J. A. del Alamo, Tech. Dig.- Int. Electron Devices Meet. 2006.
3. S. Datta, T. Ashley, R. Chau, K. Hilton, R. Jefferies, T. Martin, and T. J. Phillips, Tech. Dig. - Int. Electron Devices Meet. 2005, 783.
4. J. Robertson, J. Vac. Sci. Technol. B **18**, 1785 (2000).
5. P. W. Peacock and J. Robertson, J. Appl. Phys. **92**, 4712 (2002).
6. E. Cicerrella, J. L. Freeouf, L. F. Edge, D. G. Schlom, T. Heeg, J. Schubert, and S. A. Chambers, J. Vac. Sci. Technol. A **23**, 1676 (2005).
7. L. F. Edge, D. G. Schlom, S. A. Chambers, E. Cicerrella, J. L. Freeouf, B. Holländer, and J. Schubert, Appl. Phys. Lett. **84**, 726 (2004).
8. P. Sivasubramani, M. J. Kim, B. E. Gnade, R. M. Wallace, L. F. Edge, D. G. Schlom, H. S. Craft, and J.-P. Maria, Appl. Phys. Lett. **86**, 201901 (2005).
9. L. F. Edge, D. G. Schlom, R. T. Brewer, Y. J. Chabal, J. R. Williams, S. A. Chambers, C. Hinkle, G. Lucovsky, Y. Yang, S. Stemmer, M. Copel, B. Holländer, and J. Schubert, Appl. Phys. Lett. **84**, 4629 (2004).
10. J.M. Panfile, A.R. Fisher, S. Hanscom, and D.G. Schlom (unpublished).
11. N. Goel, P. Majhi, W. Tsai, M. Warusawithana, D.G. Schlom, M.B. Santos, J.S. Harris, and Y. Nishi, submitted to Appl. Phys. Lett.
12. S. P. Kowalczyk, D. L. Miller, J. R. Waldrop, P. G. Newman, and R. W. Grant, J. Vac. Sci. Technol. **19**, 255 (1981).
13. W. H. Schulte, B. W. Busch, E. Garfunkel, T. Gustafsson, and G. Schiwietz, Nucl. Instrum. Meth. B **183**, 16 (2001).
14. R. M. Tromp, M. Copel, M. C. Reuter, and M. Horn von Hoegen, and J. Speidell, Rev. Sci. Instrum. **62**, 2679 (1991).
15. E. A. Kraut, R. W. Grant, J. R. Waldrop, and S. P. Kowalczyk, Phys. Rev. Lett. **44**, 1620 (1980).
16. E. A. Kraut, R. W. Grant, J. R. Waldrop, and S. P. Kowalczyk, Phys. Rev. B **28**, 1965 (1983).
17. Z. Liu, Y. Sun, F. Machuca, P. Pianetta, W. E. Spicer, and R. F. W. Pease, J. Vac. Sci. Technol. B **21**, 1953 (2003).
18. S. A. Chambers, Y. Liang, Z. Yu, R. Droopad, J. Ramdani, and K. Eisenbeiser, Appl. Phys. Lett. **77**, 1662 (2000); S. A. Chambers, Y. Liang, Z. Yu, R. Droopad, and J. Ramdani, J. Vac. Sci. Technol. A **19**, 934 (2001).
19. S. Miyazaki, J. Vac. Sci. Technol. B **19**, 2212 (2001); S. A. Chambers, T. Droubay, T. C. Kaspar, and M. Gutowski, J. Vac. Sci. Technol. B **22**, 2205 (2004).
20. X. B. Lu, Z. G. Liu, Y. P. Wang, Y. Yang, X. P. Wang, H. W. Zhou, and B. Y. Nguyen, J. Appl. Phys. Lett. **94**, 1229 (2003); A. D. Li, Q. Y. Shao, H. Q. Ling, J. B. Cheng, D. Wu, Z. G. Liu, N. B. Ming, C. Wang, H. W. Zhou, and B. Y. Nguyen, Appl. Phys. Lett. **83**, 3540 (2003).
21. S.-G. Lim, S. Kriventsov, T. N. Jackson, J. H. Haeni, D. G. Schlom, A. M. Balbashov, R. Uecker, P. Reiche, J. L. Freeouf, and G. Lucovsky, J. Appl. Phys. **91**, 4500 (2002)